Iran Polym J (2015) 24:871–881
DOI 10.1007/s13726-015-0375-7

ORIGINAL PAPER

Strain rate sensitivity of toughened epoxy

Saurabh Chaudhary[1,2] · Nahid Iqbal[2] · Vikas Mangla[3] · Devendra Kumar[2] · Prasun Kumar Roy[1]

Received: 30 November 2014 / Accepted: 17 August 2015 / Published online: 27 August 2015

Abstract The high strain rate behaviour of toughened epoxy is explored under compressive loadings. A cycloaliphatic epoxy was toughened using different types of preformed fillers: epoxy-coated elastomeric poly(dimethylsiloxane) (CSR) and thermoplastic polystyrene microspheres. The toughening ability of the fillers was quantified in terms of improvement in izod impact strength. Our studies revealed that the disadvantages associated with liquid rubber toughening, especially lowering of the glass transition temperature (T_g) and storage modulus, could be overcome by using poly(dimethylsiloxane) (PDMS) microspheres. The izod impact strength increased by 33 % upon addition of 3 % w/w amino-polystyrene microspheres, and ~125 % upon introduction of CSR (5 % w/w). High strain rate studies performed using split Hopkinson pressure bar revealed that the compressive strength of epoxy and the toughened compositions were significantly enhanced at high strain rates (~10^3 s^{-1}) compared with that at quasi-static loading conditions (~10^{-1} s^{-1}). The effect of filler type on the strain rate sensitivity of the base polymer was established by comparing the property enhancement factor (PEF). Although introduction of elastomeric microspheres led to a lower compressive strength of epoxy, the PEF associated with the rubber-toughened composites was substantially higher than that with the thermoplastic-toughened analogous compositions, which was attributed to the viscous energy absorption in PDMS resulting from the dynamic rubber to glass transition at high strain rates.

Keywords High strain rate · Split Hopkinson pressure bar · Epoxy

✉ Prasun Kumar Roy
pk_roy2000@yahoo.com

[1] Centre for Fire, Explosive and Environment Safety, DRDO, Timarpur, Delhi 110054, India

[2] Department of Applied Chemistry and Polymer Technology, Delhi Technological University, Delhi 110042, India

[3] Terminal Ballistics Research Laboratory, DRDO, Chandigarh 160 030, India

Introduction

Polymeric composite materials are finding increasing usage in engineering applications, primarily because of their low specific weight and production costs. In this context, epoxy resins constitute the most common matrix material for preparation of polymeric composites. Unfortunately, conventional polyepoxides are extremely vulnerable to impact-induced damage because of their inherently cross-linked structure, thereby limiting their use in highly demanding applications. Physical toughening techniques like blending with elastomers [1–3], thermoplastics [4] and rigid particulates [5, 6] have been attempted to improve the dynamic properties of the base resin. However, the increase in toughness is usually associated with a concomitant decrease in modulus, strength and very often the resultant blends exhibit low glass transition temperatures [7].

It is to be noted that irrespective of the material employed for epoxy toughening, it is the thermodynamically and kinetically controlled process of phase separation which governs the morphology of the resultant blend and in turn defines its final properties and applications [8]. Curing of epoxy in the presence of another polymer results in the formation of phase-separated blends, a process difficult to control in fast curing compositions. Researchers worldwide are exploring techniques towards developing ways and means of controlling the blend morphology [9–11]. In this

context, an attractive alternative which has garnered much attention involves inclusion of designed preformed materials [12–14], which lead to greater improvements at comparatively lower loadings [2].

It is desirable to understand the mechanical response of materials under high strain rates, as these materials are often accidentally subjected to impact and shock loadings. Surprisingly, there seems to be limited work in the area of high strain rate characterization of polymer composites, although ample studies on the quasi-static mechanical properties are available.

In addition, it is extremely important to be cognizant of the effect of type of toughening fillers on the strain rate sensitivity of the base matrix. In our previous papers, we have demonstrated the ability of functionalized polystyrene [4] and silicone microspheres [15] as effective thermoplastic and elastomeric fillers towards epoxy toughening. The fillers, however, necessitated suitable treatment to improve their interaction with the epoxy matrix. In this study, we attempt to understand the effect of these fillers on the mechanical response of the base matrix under dynamic compressive loading conditions. Increasing the strain rate led to substantial changes in the characteristic mechanical properties of epoxy, which was followed by quantification of "property change factor", defined as the ratio of the property at high strain rate loading to that under quasi-static conditions [16].

Experimental

Materials

Epoxy resin (Ciba Geigy, Araldite CY 230; epoxy equivalent 200 eq g^{-1}, Basel, Switzerland) and hardener (HY 951; amine content 32 eq kg^{-1} Basel, Switzerland) were used as received. Styrene (AR, E. Merck, KGaA, Dermstadt, Germany) was washed with 10 % aqueous sodium hydroxide to remove the inhibitor, followed by washing with water and drying over anhydrous sodium sulphate. Poly(vinyl alcohol) (PVA) (M_w: 14,000 g mol^{-1}, Central Drug House, Mumbai, India) and benzoyl peroxide (AR, Central Dug House, Mumbai, India) were used without any further purification. Silicone resin (Elastosil M4644) and the platinum-based hardener were obtained from Wacker, Germany. Double distilled water was used throughout the course of this study.

Preparation of amine-functionalized polystyrene microspheres

The preparation of polystyrene microspheres by suspension polymerization process has been detailed in our previous papers [4]. In brief, a solution of styrene (in toluene) and benzoyl peroxide (0.05 % w/v styrene) was introduced into a reaction vessel containing aqueous solution of PVA (1.5 % w/v) and the polymerization reaction was allowed to proceed at 80 ± 2 °C under inert atmosphere for 8 h under stirring, after which the reaction mixture was cooled and filtered. The microspheres were nitrated with 5:2 v/v mixture of sulphuric acid and nitric acid at 60 °C on a controlled water bath for 1 h. Nitro-polystyrene microspheres (NPS) were washed with distilled water, dried under vacuum and reduced to amino-polystyrene (APS) with a mixture of tin(II) chloride and concentrated hydrochloric acid in 50 mL ethanol for 12 h at 90 °C [17]. The product was filtered, washed first with distilled water and then alkali (2 M NaOH) to recover the free amino derivative.

Preparation of core/shell elastomeric microspheres

The silicone core was prepared by suspension polymerization process as per the procedure detailed in our previous papers [15, 18, 19]. In brief, the vinyl-terminated siloxane macromonomer and hardener were introduced into a reaction vessel through a hypodermic syringe into an aqueous PVA solution (1.5 % w/v). The curing reaction was allowed to proceed under inert atmosphere at 45 °C under continuous stirring for 8 h, after which the reaction mixture was cooled and filtered.

The microspheres were coated with epoxy in a separate step to prepare core/shell rubber (CSR). For this purpose, a mixture of PDMS microspheres (15 g) and epoxy resin (7 g) was ultrasonicated for 15 min prior to addition of stoichiometric amounts of hardener. The mixture was diluted with small amounts of chloroform (5 mL), and the slurry was slowly introduced into a reactor containing aqueous PVA solution being stirred under the conditions mentioned previously.

Preparation of epoxy composites

Microspheres were sieved to obtain uniform particles, which were then added to the epoxy resin in required amounts (1–7 % w/w) followed by ultrasonication of the resulting mixture for 30 min at 33 kHz. Triethylene tetraamine hardener was added to the mixture (13 phr) to achieve an amine:epoxide stoichiometry of 1:1 and ultrasonicated for another 15 min to remove the entrapped air bubbles. The suspension was transferred to cylindrical greased silicone moulds (12 mm diameter × 5 mm height), where the curing reaction was allowed to proceed for 24 h at 30 °C. Prior to testing, the faces of the cylindrical specimens were polished with 240 grit-size silicon carbide abrasive paper followed by polishing with 600 grit-size emery paper. Neat epoxy specimens were also prepared in a

similar manner and the samples have been designated as EP followed by their concentration and by the type of microsphere used for their preparation, i.e. 'APS' denotes polystyrene beads functionalized with amino groups and CSR denotes epoxy-coated core–shell poly(dimethylsiloxane) beads. For example, EP3APS refers to a thermoplastic-toughened epoxy containing amino-polystyrene (3 % w/w), and EP5CSR refers to rubber-toughened epoxy containing core–shell poly(dimethylsiloxane) beads (5 %w/w).

Mechanical properties

The quasi-static compressive mechanical properties of composites were determined by subjecting the cylindrical specimens to a compressive load, at cross head speed of 50 mm min^{-1} corresponding to a strain rate of 0.17 s^{-1}, using a universal testing system (International Equipments, Mumbai, India) at 30 °C. The notched izod impact strength of the specimens was determined as per ASTM D 256 using an impact strength testing machine (International Equipments, Mumbai, India). For each composition, at least five identical specimens were tested and the average results along with the standard deviation were reported.

The surface morphology of samples was studied using a scanning electron microscope (Zeiss EVO MA15, Oberkochen, Germany) under an acceleration voltage of 1 kV. Samples were mounted on aluminium stubs and sputter coated with gold and palladium (10 nm) using a sputter coater (Quorum- SC7620, Oberkochen, Germany) operating at 10–12 mA for 120 s.

High strain rate studies

The mechanical response of the samples under high strain rates was established using a split Hopkinson pressure bar (SHPB). The setup (Fig. 1) at Terminal Ballistic Research Laboratory (TBRL), Chandigarh, comprises two high-strength maraging steel with yield strength 1750 MPa, diameter 20 mm and length 2000 mm. A projectile (300 mm length and 20 mm diameter) was shot by a pressure gun to hit the cylindrical samples sandwiched between the two bars to produce different strain rates varying between 1096 and 2900 s^{-1} [20]. Strain gauges of 120 Ω, 90° tee rosette precision stain gauges designated as EA-06-125TM-120 were used. For wave shaping, a 1.5 mm OFHC copper wave shaper was used.

As the front disc of the propelling mechanism impacts onto the disc mounted on the incident bar, an elastic stress pulse is generated and travels along the incident bar. When the pulse reaches the specimen, which is sandwiched between the incident and transmitter bars, part of the stress pulse is reflected and the remaining part is transmitted through the specimen to the transmitter bar. The strain gauges mounted at the centre of incident and transmitter bars provide the time-resolved measure of the signals. The strain gauge mounted on the incident bar measures incident and reflected pulses, whereas the strain gauge mounted on the transmitter bar measures the transmitted pulse. The strain gauges are installed midway on the incident and transmitter bars to avoid overlapping of the signals. During loading, the specimen undergoes dynamic elastic–plastic deformation. From the reflected pulse, the strain rate applied and the strain in the specimen are estimated, whilst the transmitted pulse provides a measure of the stress. The reflection of the pulse from the interface of the bar and specimen is due to the impedance mismatch between the bar and the specimen [20].

The basic principle of SHPB is based on one-dimensional wave propagation in elastic bars, which can ideally be considered to be of infinite length and negligible diameter. In all the experiments, cylindrical specimens with length to diameter (*L*/*D*) ratio of 0.41 were used, with the diameter of the specimen being 12 mm. This ensured the impact on full cross section of the specimen and also permitted the specimen to expand along the radial direction within the cross-sectional area of the bars after the compressive load was applied. The deformation history within the sample was obtained by recording the strain on the incident and transmitter bars from the strain gauges with the help of an amplifier and oscilloscope. From these signals and using one-dimensional wave propagation theory, strain rate versus time, strain versus time, stress versus time and stress versus strain plots in the specimen are obtained. Further, force history at the interface between the specimen and the incident bar (F1) and the specimen and the transmitter bar (F2) is also obtained. The analytical relations to calculate strain rate, strain and stress as a function of time in the specimen in SHPB testing are as follows:

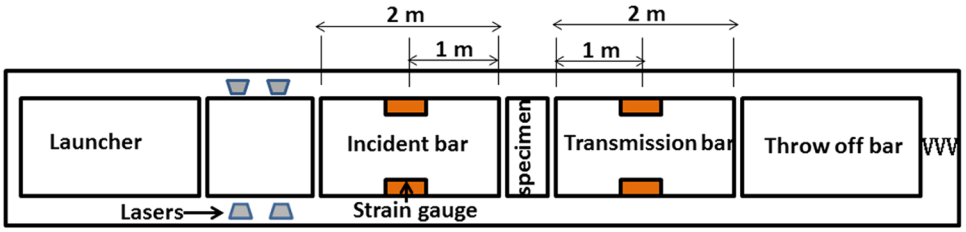

Fig. 1 Schematic representation of the compressive SHPB experiment

$$\text{Strain rate, } \dot{\varepsilon}_s(t) = \left(\frac{2C_0}{l_s}\right)\varepsilon_R(t),$$

$$\text{Average strain, } \varepsilon_s(t) = \pm\left(\frac{2C_0}{l_s}\right)\int_0^t \varepsilon_R(t)\mathrm{d}t,$$

$$\text{Stress, } \sigma_s(t) = \pm E\frac{A_B}{A_S}\varepsilon_T(t),$$

where C_0 is the elastic wave velocity in the bars, l_S the specimen gauge length, A_B the cross-sectional area of the bars, A_S the cross-sectional area of the specimen, E the Young's modulus of the bars, ε_R the reflected strain pulse, ε_T the transmitted strain pulse and t the time duration.

Results and discussion

A cycloaliphatic epoxy resin was toughened using two different classes of preformed additives, namely elastomeric and functionalized polystyrene microspheres. The effect of these fillers on the mechanical response of the base resin was studied under different strain rate regimes under compressive loadings.

Epoxy toughening

SEM images of silicone and amino-polystyrene microspheres are presented in Fig. 2. It can be seen that in comparison to PDMS, the surface of APS microspheres is relatively rougher and the cracked surface emerges as a result of nitration of the other smooth polystyrene surface. The effect of introduction of both types of fillers on the toughening ability of epoxy resin has been discussed in our previous papers [4, 15].

No significant reduction in the T_g values of the base polymer was observed by introduction of the microspheres, and the damping tan δ traces were found to overlap in the DMA traces (Fig. 3). This is in contrast with the results reported on epoxy blends with organic liquid rubbers, e.g. CTBN, where significant reduction in T_g has been reported [21]. Our studies clearly highlight the benefit of employing preformed elastomeric microspheres as impact modifiers as the second phase remains phase separated, in view of which their plasticizing action is practically negligible. Neat epoxy exhibits a glass transition of 66 °C (tan δ peak) and storage modulus of 3.3×10^{10} Pa (at 30 °C), which remain practically unaffected upon addition of either type of filler. The additional hump at 110 °C in EP3APS corresponds to the T_g of amorphous PS phase, which suggests the existence of completely phase-separated fillers without any evidence of plasticizing action.

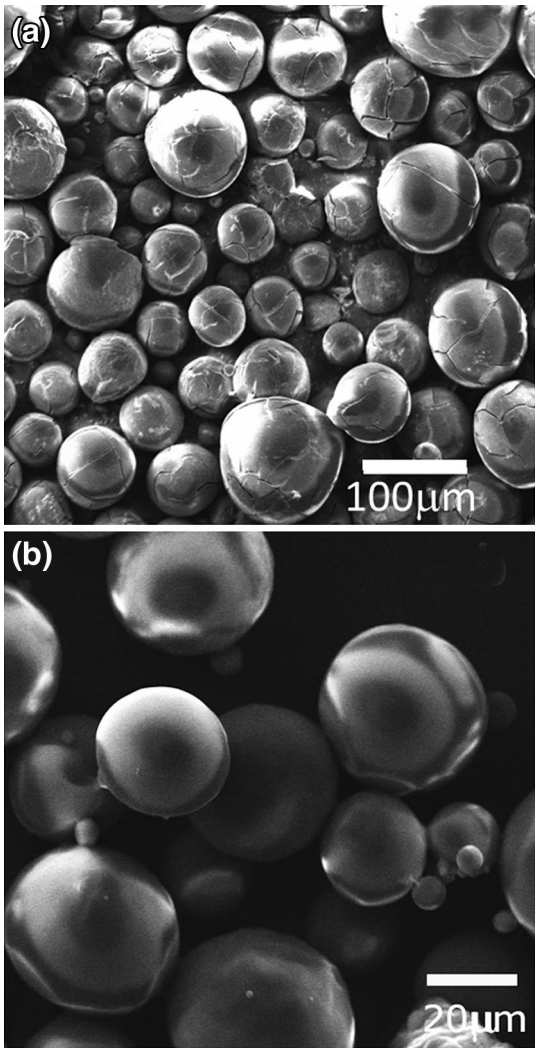

Fig. 2 SEM images of **a** amino-polystyrene, and **b** PDMS microspheres

The effect of either type of filler on the impact strength of the base epoxy resin is presented in Fig. 4. The izod impact strength increases from 24 J m^{-1} (unmodified epoxy) to 32 J m^{-1} on addition of 3 % w/w APS, corresponding to a ~33 % increase. In comparison, the impact strength was substantially higher (~125 %), when rubbery microspheres were employed as the preformed filler, nonetheless at slightly higher loadings (5 % w/w). Since the extent of improvement in the toughness was maximum at 3 % APS loading and 5 % PDMS loading, high strain rate testing was performed only on these compositions. Similar increase in the toughness at such low loadings has been reported earlier [22]; however, CSR-based epoxy systems exhibit additional advantage of being useable at higher temperatures in view of the exceptional thermal stability of silicones.

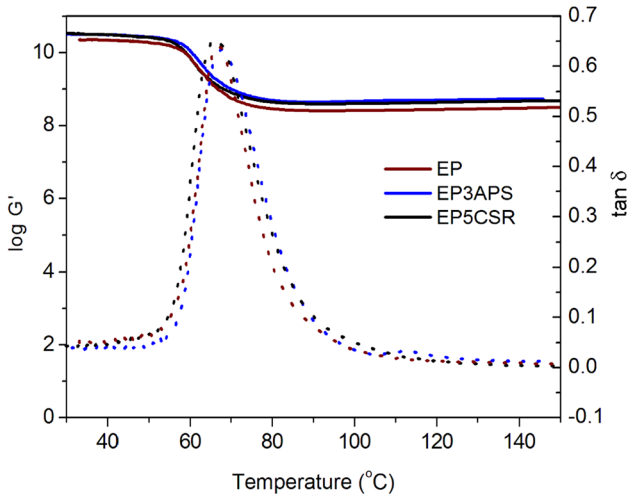

Fig. 3 Variation of storage modulus and loss factor as a function of temperature

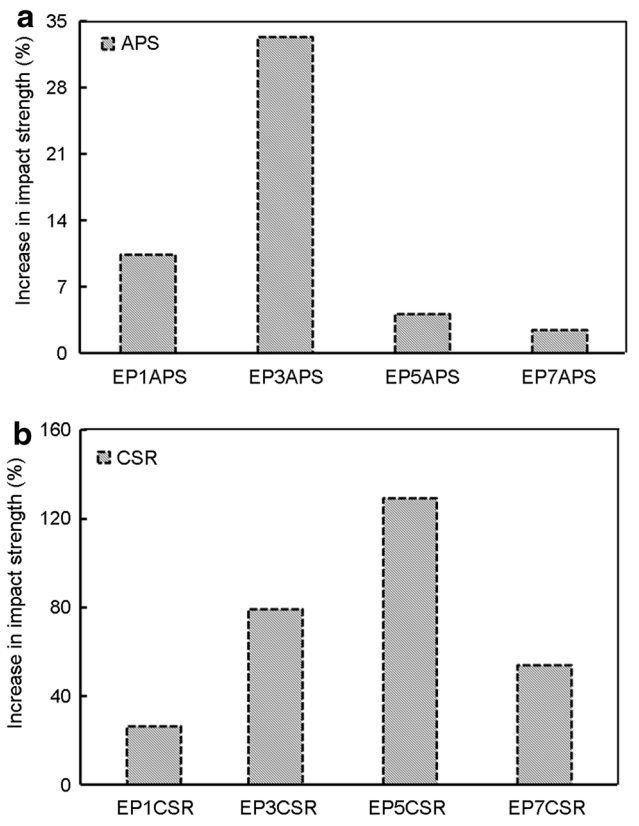

Fig. 4 Increase in impact strength due to introduction of **a** elastomeric and **b** thermoplastic microspheres

The primary criterion which needs to be fulfilled by the preformed additives to exhibit their full potential as impact modifiers is their random dispersion in the matrix as a well-separated phase. The amino groups on the surface of functionalized polystyrene and the layer of epoxy in the CSR strongly interact with the epoxy during the curing process, which leads to their good dispersion in the matrix, and the same is evident from the SEM images. However, with increased loadings, agglomeration of these microspheres was observed which was responsible for the decrease in the mechanical properties.

Fractography was performed to understand the toughening mechanisms underlying the improved toughness of the filled epoxy composites. The SEM images of the fractured surface are presented in Fig. 5. Characteristic features, particularly crack pinning and microcracking, are clearly visible on the fracture surface of thermoplastic-toughened epoxy (Fig. 5a, b), which reportedly absorb a substantial amount of impact energy [23]. Interestingly, these features are not observed on the surface of rubber-filled composites, where features associated with rubber cavitation are visible (Fig. 5c, d) [24]. It can be presumed that mechanical loading in rubber-toughened compositions results in dilation of the plastic region surrounding the rubbery phase, leading to its cavitation from within. The cavitation process relieves the plane strain constraint from the surrounding matrix and permits a significant amount of plastic deformation. Another mechanism which can be used to explain the toughened nature of these composites is that of particle yielding-induced shear banding, a process which starts with the yielding of the rubber, thereby directing significant stress concentration away from the matrix [1, 25].

High strain rate behaviour

The effect of increasing strain rate on the stress–strain behavior of samples was quantified using split Hopkinson pressure bar. The details of SHPB working are widely available in the literature [16, 26]. The SHPB setup consists of two long bars, namely, input bar and output bar that sandwich a short specimen. High gas pressure acts as a source of impact, which propels a projectile striking an end of the input bar. As a result, a compressive stress wave is generated which travels towards the specimen. Upon hitting the specimen, a fraction of the stress is transmitted as a compression wave, which eventually reaches the output bar, while another wave is reflected back towards the input bar in a tensile mode. Usually, an irreversible plastic deformation results in the specimen due to this process, which lasts for a very short duration (<1 s). The wave signal measurements are performed using strain gauges attached on the input and output bars.

To assess the accuracy of the SHPB apparatus, a pretest calibration was performed, during which the input and output bars were pressed together without the sandwiched specimen. The strain gauge signals obtained on the oscilloscope during calibration are presented in Fig. 6. Channel

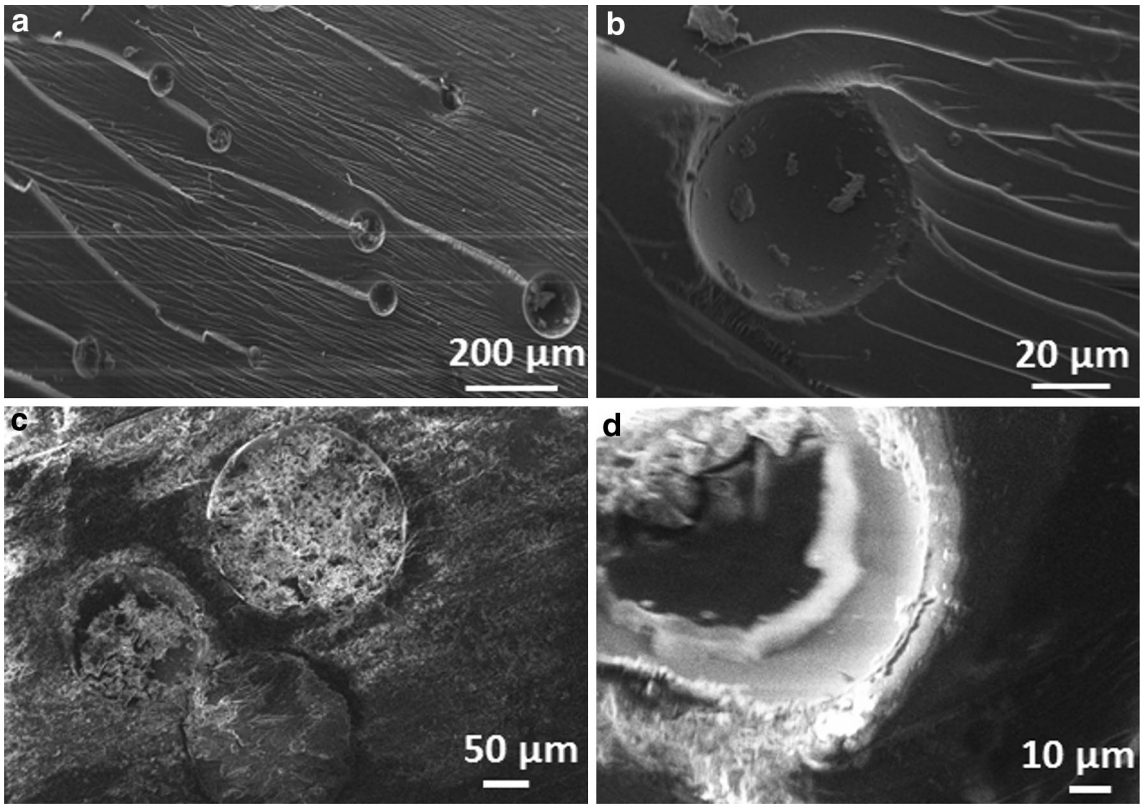

Fig. 5 SEM image of fractured surface of composites showing evidence of **a** crack pinning, **b** microcracking in APS-toughened epoxy and **c**, **d** rubber cavitation in PDMS-toughened epoxy

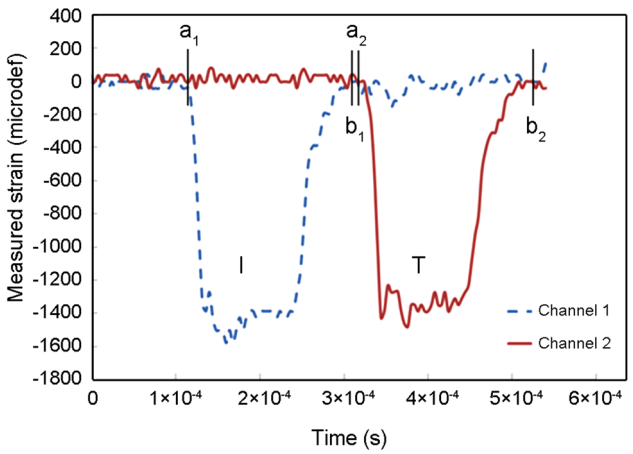

Fig. 6 Strain versus time signals during pre-testing calibration

1 and Channel 2 refer to the strain gauge output mounted on the incident bar and transmitter bar, respectively. Here, I is the incident pulse with pulse duration equal to a_1a_2 and T is the transmitted pulse with pulse duration equal to b_1b_2. The absence of reflected pulse and the near similarity of amplitude and duration of incident and transmitted pulses ensured perfect alignment and friction-free functioning of the SHPB apparatus and hence high strain rate testing could be conducted subsequently. The measured strain associated with neat epoxy (EP) and toughened compositions, i.e. EP3APS and EP5CSR, are presented in Fig. 7. It can be seen that the duration of incident and reflected signals are nearly the same for epoxy as well as its composites (192 µs).

The force/time plots obtained from the strain gauge signals for neat epoxy are also included in Fig. 7. Force history on the incident bar has been plotted based on strain gauge signal '$I + R$', and the force history on the transmitter bar has been plotted based on strain gauge signal 'T' which will be referred to as F1 and F2 for further discussion. Force F1 acts on the interface between the incident bar and the specimen and force F2 acts on the interface between the transmitter bar and the specimen. The strain gauge data were used to generate the stress strain curve, which in turn was used to arrive at the compressive strength and modulus. True stress–strain curves at different strain rates are presented in Fig. 8.

Only a single curve for each case is presented to ease the comparison of the results. It can be seen that the mechanical response of composites under uniaxial compression exhibits great strain rate dependent characteristics. Under

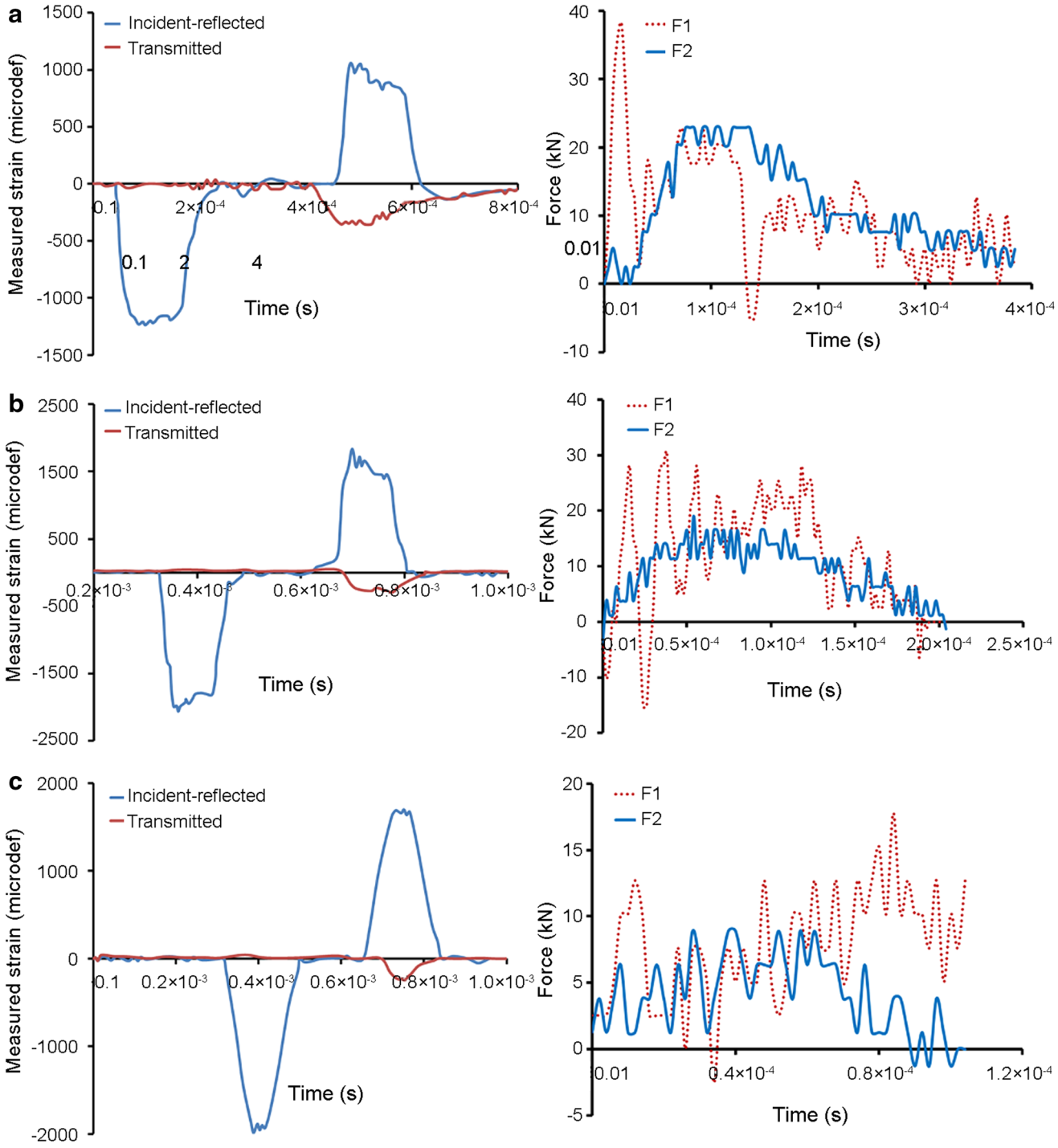

Fig. 7 Representative oscilloscope signals and force histories obtained during dynamic compressive experiments: **a** neat epoxy, **b** EP3APS and **c** EP5CSR

quasi-static conditions, the stress–strain curve of epoxy as well as the composites exhibited similar behavior: a linear elastic response in the initial loading stage, followed by minor nonlinear behavior up to the yielding point, followed by an insignificant strain softening. Similar behavior has been reported earlier for polycarbonate [27], polypropylene [28], epoxy composites [16, 29, 30] as well as nanocomposites [31].

It is to be noted that under high strain compressive testing, the strain rate is not constant during the initial stages of loading. Therefore, the Young's modulus obtained based on the strain gauge data in this region is inexact. The variations

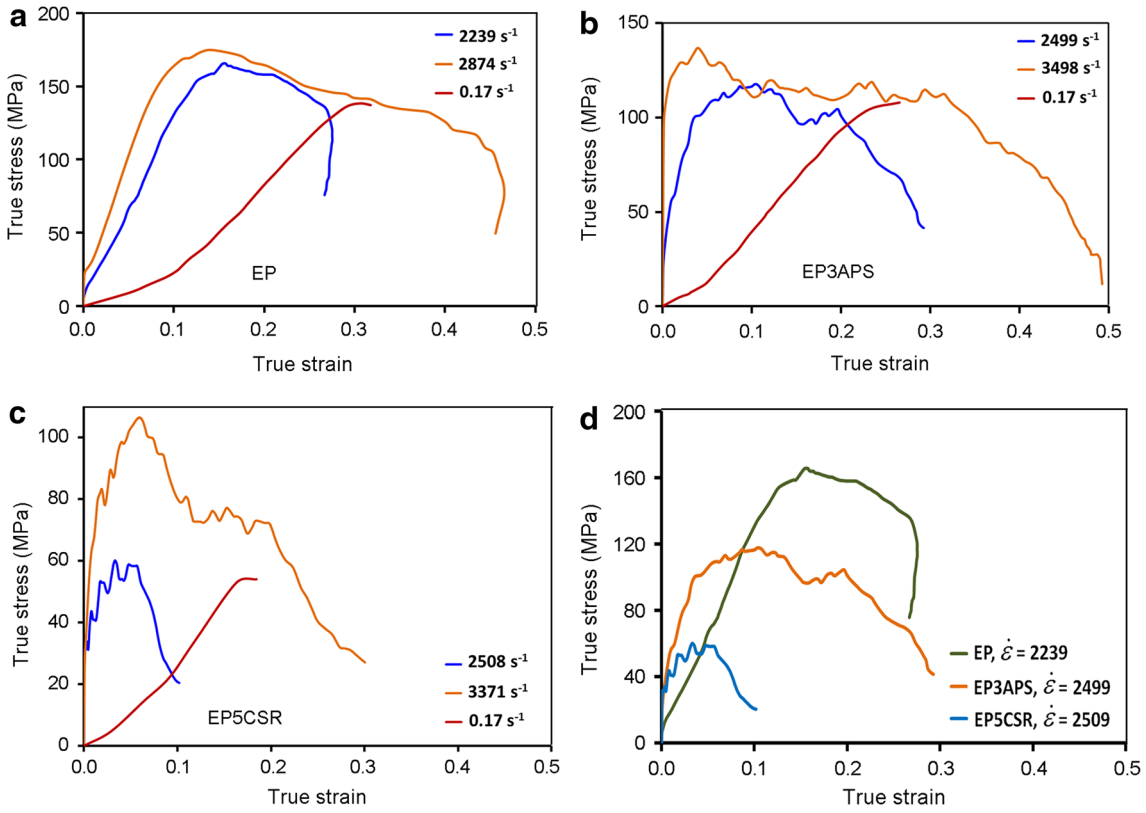

Fig. 8 Effect of strain rate on the compressive stress–strain behaviour of epoxy and toughened compositions: **a** EP, **b** EP3APS, **c** EP5CSR and **d** the effect of filler type on the stress strain profile at similar strain rates

of strain rate and stress versus time for the representative samples are presented in Fig. 9. It can be seen that the strain rate variation is relatively less beyond the rising time and hence the stress–strain behaviour obtained beyond the rising time of the pulse can be considered to be the actual behaviour of the material. As an approximation, Young's modulus was determined by joining the origin to a point in the stress–strain curve associated with the maxima in the strain rate versus time profile [16], with the value obtained being indicative of the lower bound of Young's modulus.

Increasing the strain rate led to substantial changes in characteristic mechanical properties, which was followed by quantifying the increase in the "property enhancement factor" (PEF), defined as the ratio of the property at high strain rate loading to that under quasi-static conditions (Table 1) [29]. The change in the mechanical response upon increasing the strain rate is attributed to the reduction in the molecular mobility of polymer chains, which increases its inherent stiffness [32].

It is particularly interesting to note the effect of the filler type (thermoplastic and elastomeric) on the strain rate sensitivity of epoxy. In general, both types of fillers affect the mechanical properties, which are more pronounced for rubber-toughened compositions.

The compressive modulus of unfilled epoxy was found to increase from 464 MPa under quasi-static conditions to 1875 MPa at 2874 s^{-1}, corresponding to a PEF of 4.04. The corresponding increase in the flow stress (at 10 % true strain) is from 138 MPa under quasi-static conditions to ~175 MPa (PEF = 1.26).

For EP3APS, the flow stress increased from 108 MPa under quasi-static conditions to ~151 MPa (ε = 3598 s^{-1}) (PEF = 1.40). In comparison, the compressive modulus increased from 367 to 4500 MPa at 3371 s^{-1} corresponding to a PEF of 16.8 for rubber-toughened epoxy (EP3P-DMS). Also, the flow stress of the composite increased to ~105 MPa from 49 MPa under quasi-static conditions, corresponding to a PEF of 2.14.

It has been reported that PDMS exhibits extremely low "calorimetric glass transition temperature (T_g)" of the order of −113 °C [33]. At the molecular level, this rubbery- to glassy-state transition is related with the loss of mobility of the local chain segments. At T_g, the second-order derivatives of Gibbs free energy of PDMS (e.g. specific heat) undergo an irregular change, while the first-order derivative (e.g. volume) remains practically unaltered. The low T_g of elastomeric PDMS grants significant segmental mobility to the polymeric chain at ambient temperatures. Interestingly,

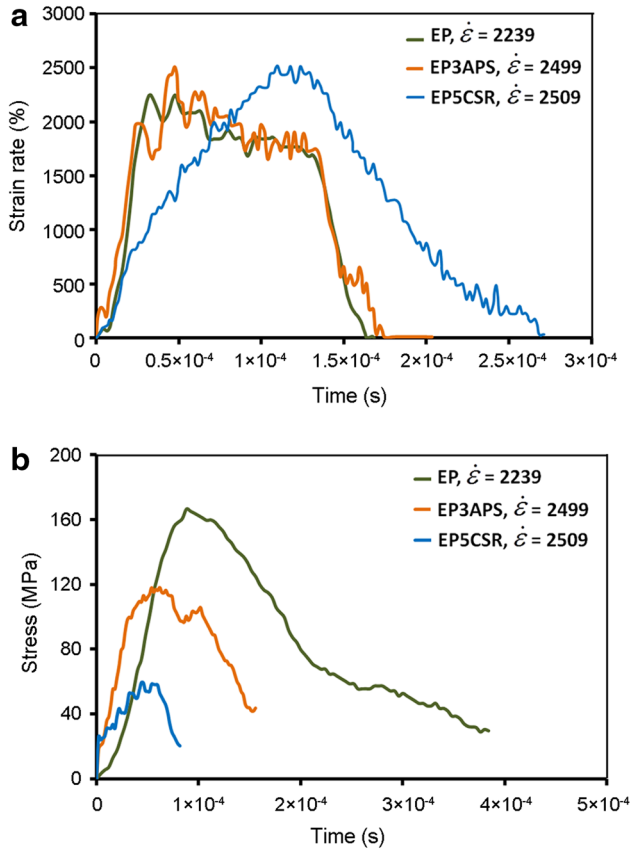

Fig. 9 **a** Strain rate versus time and **b** stress versus time curve for epoxy and toughened compositions at $\varepsilon = 2239–2508\ s^{-1}$

this loss in mobility also takes place at temperatures higher than T_g, in the event of the strain rates becoming comparable to the vibrational frequencies of the chain segments. This confines the large-scale rearrangements of the polymer chains during deformation and the material transitions from rubbery to the glassy state, a phenomenon associated with an increase in the modulus.

This can be used to explain the higher strain rate sensitivity of rubber-toughened composites. This was further confirmed by previous studies on strain rate sensitivity of rubbers [34, 35]. In a previous study, the flow stress and modulus of polyurethane-based elastomer were reported to increase by 22.56 and 8.15, respectively (strain rate of 3800 s^{-1}) [34]. In a separate study, the PEF (X_c) of polyurea has been reported to be 3.14 at 2250 s^{-1} [35]. It has been reported that the T_g of polyurea increases with increasing strain rate and undergoes brittle failure at high strain rates [36]. It is in this context that polyurea is being advocated as a material of choice for retrofitting applications in blast mitigating coatings [37, 38].

On the other hand, the glass transition temperature of the thermoplastic PS microspheres is much higher than room temperature (T_g = 110 °C), which leads to its existence in the glassy state at ambient temperatures. Hence, the viscous energy absorption in PDMS due to rubber–glass transition is not possible in PS. Consequently, the effect of its inclusion of PS on the strain rate sensitivity of epoxy is relatively less pronounced as compared to rubber-toughened compositions.

Table 1 Mechanical response of epoxy composites under high strain rate

Material	Strain rate (s^{-1})	X_c (MPa)	E_c (MPa)	PEF	
				(X_c)	(E_c)
Epoxy	0.17	138	464	–	–
	2239	166	1471	1.19	3.17
	2874	175	1875	1.26	4.04
EP3APS	0.17	108	474	–	–
	2288	126	5000	1.17	8.17
	3598	151	8000	1.40	12.26
EP5CSR	0.17	49	367	–	–
	2508	59	3000	1.20	10.54
	3371	105	4500	2.14	16.87

PEF property enhancement factor; X_c and E_c refer to stress and modulus, respectively

This is in line with previous studies on the high strain rate behaviour of unfilled thermoplastics, e.g. poly(methyl methacrylate) (PMMA) [39, 40], polycarbonate [27, 41] and HDPE [42], where a comparison with the behaviour of elastomers reveals weaker strain rate sensitivity of the thermoplastics. It can be seen from Table 1 that the compressive modulus of APS-filled epoxy increases from 474 MPa under quasi-static conditions to 8000 MPa at 3598 s^{-1}, corresponding to a PEF of 12.26, which is in line with the existing literature in this field.

Conclusion

Two types of preformed fillers were explored towards toughening of a representative cycloaliphatic epoxy resin: thermoplastic (amino-polystyrene) and elastomeric (epoxy-coated PDMS) microspheres. The compressive properties of toughened epoxy were presented under high strain rate loading. The overall observations are:

- Introduction of either type of filler increased the impact strength of the base resin, the effect being more pronounced for rubber-toughened compositions.
- Compressive strength was found to increase with increasing strain rate.
- Compressive modulus also increased at high strain rate loading compared to that under quasi-static conditions.

- The effect of strain rate on the compressive properties was more pronounced in the case of rubber-toughened epoxy as compared to thermoplastic-toughened analogue.

Quantitative data are presented in the paper.

Acknowledgments The authors are thankful to the Director, CFEES, and the Director, TBRL, for taking keen interest and providing the laboratory facilities.

References

1. Bagheri R, Marouf BT, Pearson RA (2009) Rubber-toughened epoxies: a critical review. J Macromol Sci Part C Polym Rev 49:201–225
2. Pearson RA, Yee AF (1991) Influence of particle size and particle size distribution on toughening mechanisms in rubber-modified epoxies. J Mater Sci 26:3828–3844
3. Akbari R, Beheshty MH, Shervin M (2013) Toughening of dicyandiamide-cured DGEBA-based epoxy resins by CTBN liquid rubber. Iran Polym J 22:313–324
4. Chaudhary S, Surekha P, Kumar D, Rajagopal C, Roy PK (2015) Amine-functionalized poly(styrene) microspheres as thermoplastic toughener for epoxy resin. Polym Compos 36(174):183
5. Roy PK, Ullas AV, Chaudhary S, Mangla V, Sharma P, Kumar D, Rajagopal C (2013) Effect of SBA-15 on the energy absorption characteristics of epoxy resin for blast mitigation applications. Iran Polym J 22:709–719
6. Norman DA, Robertson RE (2003) Rigid-particle toughening of glassy polymers. Polymer 44:2351–2362
7. Chaudhary S, Parthasarathy S, Kumar D, Rajagopal C, Roy PK (2014) Graft-Interpenetrating polymer networks of epoxy with polyurethanes derived from poly(ethyleneterephthalate) waste. J Appl Polym Sci. doi:10.1002/app.40490
8. Hoppe CE, Galante MJ, Oyanguren PA, Williams RJJ, Girard-Reydet E, Pascault JP (2002) Transparent multiphasic polystyrene/epoxy blends. Polym Eng Sci 42:2361–2368
9. Zucchi IA, Galante MJ, Williams RJJ (2005) Comparison of morphologies and mechanical properties of crosslinked epoxies modified by polystyrene and poly(methyl methacrylate)) or by the corresponding block copolymer polystyrene-*b*-poly(methyl methacrylate). Polymer 46:2603–2609
10. Bhattacharyya AR, Ghosh AK, Misra A, Eichhorn KJ (2005) Reactively compatibilised polyamide 6/ethylene-co-vinyl acetate blends: mechanical properties and morphology. Polymer 46:1661–1674
11. Barlow JW, Paul DR (1984) Mechanical compatibilization of immiscible blends. Polym Eng Sci 24:525–534
12. Ratna D, Banthia AK (2004) Rubber toughened epoxy. Macromol Res 12:11–21
13. Hayes BS, Seferis JC (2001) Modification of thermosetting resins and composites through preformed polymer particles: a review. Polym Compos 22:451–467
14. Levita G, Marchetti A, Lazzeri A (1991) Toughness of epoxies modified by preformed acrylic rubber particles. Makromolekulare Chemie Macromol Symp 41:179–194
15. Roy P, Iqbal N, Kumar D, Rajagopal C (2014) Polysiloxane-based core-shell microspheres for toughening of epoxy resins. J Polym Res 2:1–9
16. Naik NK, Shankar PJ, Kavala VR, Ravikumar G, Pothnis JR, Arya H (2011) High strain rate mechanical behavior of epoxy under compressive loading: experimental and modeling studies. Mater Sci Eng A 528:846–854
17. Roy PK, Rawat AS, Rai PK (2003) Synthesis, characterisation and evaluation of polydithiocarbamate resin supported on macroreticular styrene–divinylbenzene copolymer for the removal of trace and heavy metal ions. Talanta 59:239–246
18. Manju RP, Ramanan A, Rajagopal C (2014) Core-shell polysiloxane-MOF 5 microspheres as a stationary phase for gas–solid chromatographic separation. RSC Adv 4:17429–17433
19. Roy P, Iqbal N, Kumar D, Rajagopal C (2014) Rubber toughening of unsaturated polyester with core–shell poly(siloxane)-epoxy microspheres. Polym Bull 71:2733–2748
20. Jindal P, Pande S, Sharma P, Mangla V, Chaudhury A, Patel D, Singh BP, Mathur RB, Goyal M (2013) High strain rate behavior of multi-walled carbon nanotubes–polycarbonate composites. Compos Part B Eng 45:417–422
21. Russell B, Chartoff R (2005) The influence of cure conditions on the morphology and phase distribution in a rubber-modified epoxy resin using scanning electron microscopy and atomic force microscopy. Polymer 46:785–798
22. Affdl JCH, Kardos JL (1976) The Halpin–Tsai equations: a review. Polym Eng Sci 16:344–352
23. Kinloch AJ, Yuen ML, Jenkins SD (1994) Thermoplastic-toughened epoxy polymers. J Mater Sci 29:3781–3790
24. Chen J, Kinloch AJ, Sprenger S, Taylor AC (2013) The mechanical properties and toughening mechanisms of an epoxy polymer modified with polysiloxane-based core-shell particles. Polymer 54:4276–4289
25. Chen T, Jan Y (1991) Toughening mechanism for a rubber-toughened epoxy resin with rubber/matrix interfacial modification. J Mater Sci 26:5848–5858
26. Shim J, Mohr D (2009) Using split Hopkinson pressure bars to perform large strain compression tests on polyurea at low, intermediate and high strain rates. Int J Impact Eng 36:1116–1127
27. Rietsch F, Bouette B (1990) The compression yield behaviour of polycarbonate over a wide range of strain rates and temperatures. Eur Polym J 26:1071–1075
28. Chou SC, Robertson KD, Rainey JH (1973) The effect of strain rate and heat developed during deformation on the stress–strain curve of plastics. Exp Mech 13:422–432
29. Ravikumar G, Pothnis JR, Joshi M, Akella K, Kumar S, Naik NK (2013) Analytical and experimental studies on mechanical behavior of composites under high strain rate compressive loading. Mater Des 44:246–255
30. Pothnis JR, Ravikumar G, Joshi M, Akella K, Kumar S, Naik NK (2012) High strain rate compressive behavior of epoxy LY 556: radial constraint effect. Mater Sci Eng A 538:210–218
31. Guo Y, Li Y (2007) Quasi-static/dynamic response of SiO_2–epoxy nanocomposites. Mater Sci Eng A 458:330–335
32. Bauwens JC (1972) Relation between the compression yield stress and the mechanical loss peak of bisphenol-A-polycarbonate in the β transition range. J Mater Sci 7:577–584
33. Fragiadakis D, Pissis P (2007) Glass transition and segmental dynamics in poly(dimethylsiloxane)/silica nanocomposites studied by various techniques. J Non-Cryst Solids 353:4344–4352
34. Sarva SS, Deschanel S, Boyce MC, Chen W (2007) Stress–strain behavior of a polyurea and a polyurethane from low to high strain rates. Polymer 48(8):2208–2213
35. Roland CM, Casalini R (2007) Effect of hydrostatic pressure on the viscoelastic response of polyurea. Polymer 48:5747–5752
36. Bogoslovov RB, Roland CM, Gamache RM (2007) Impact-induced glass transition in elastomeric coatings. Appl Phys Lett 90:1–3
37. Yi J, Boyce MC, Lee GF, Balizer E (2006) Large deformation rate-dependent stress–strain behavior of polyurea and polyurethanes. Polymer 47:319–329

38. Grujicic M, Bell WC, Pandurangan B, He T (2010) Blast-wave impact-mitigation capability of polyurea when used as helmet suspension-pad material. Mater Des 31:4050–4065
39. Li Z, Lambros J (2001) Strain rate effects on the thermomechanical behavior of polymers. Int J Solids Struct 38:3549–3562
40. Mulliken AD, Boyce MC (2006) Mechanics of the rate-dependent elastic–plastic deformation of glassy polymers from low to high strain rates. Int J Solids Struct 43:1331–1356
41. Omar MF, Akil HM, Ahmad ZA (2011) Measurement and prediction of compressive properties of polymers at high strain rate loading. Mater Des 32:4207–4215
42. Briscoe BJ, Nosker RW (1984) The influence of interfacial friction on the deformation of high density polyethylene in a split Hopkinson pressure bar. Wear 95:241–262